

Proceedings of the ASME 2020
International Design Engineering Technical Conferences
and Computers and Information in Engineering Conference
IDETC/CIE2020
August 17-19, 2020, Virtual, Online

DETC2020-22643

ANALYSIS OF THE RIGID MOTION OF A DEVELOPABLE CONICAL MECHANISM

McKell Woodland

Dept. of Mathematics Brigham Young University Provo, Utah 84602 mckell.woodland@gmail.com

Erin L. Matheson

Dept. of Mathematics Brigham Young University Provo, Utah 84602 erinlmatheson@gmail.com

Jacob Greenwood

Compliant Mechanisms Research Dept. of Mechanical Engineering Brigham Young University Provo, Utah 84602 jacobgreenwood@byu.net

Michelle Hsiung

Dept. of Mathematics Brigham Young University Provo, Utah 84602 michelle88hsiung@gmail.com

C. Alex Safsten

Dept. of Mathematics Brigham Young University Provo, Utah 84602 alex.safsten@gmail.com

Denise M. Halverson

Dept. of Mathematics Brigham Young University Provo, Utah 84602 halverson@math.byu.edu

Larry L. Howell

Compliant Mechanisms Research Dept. of Mechanical Engineering Brigham Young University Provo, Utah 84602 Ihowell@byu.edu

ABSTRACT

We demonstrate analytically that it is possible to construct a developable mechanism on a cone that has rigid motion. We solve for the paths of rigid motion and analyze the properties of this motion. In particular, we provide an analytical method for predicting the behavior of the mechanism with respect to the conical surface. Moreover, we observe that the conical developable mechanisms specified in this paper have motion paths that necessarily contain bifurcation points which lead to an unbounded array of motion paths in the parameterization plane.

1 Introduction

A developable surface is a surface that can be obtained by bending, without folding, a flat surface [4]. Hence, given the inner metric, it is locally isometric to the Euclidean plane. For developable surfaces, the Gaussian curvature, or the product of the two principle curvatures, is necessarily zero [10, 13, 14]. Basic families of developable surfaces include planar, cylindrical, conical, and tangent surfaces [14].

Engineers can take advantage of the lower production costs and complexity associated with using developable surfaces in their designs. Developable surfaces designed utilizing flexible materials can be manufactured in a flat state and later transformed into their desired curved forms. Additionally, developable surfaces can often be manufactured without the heat treatment required for the production of other types of surfaces [8]. Some applications of developable surfaces include steel ship hulls, cartography, architecture, aerodynamics and texture mapping in computer graphics [1–3, 8, 15].

Because developable surfaces are commonly used in design, it is of interest to discover innovative ways to create functionality on these surfaces. Developable surfaces in \mathbb{R}^3 are ruled surfaces in the sense that they are contained in the union of a one parametric family of lines, called ruling lines. The existence of ruling lines allows the possibility of creating mechanisms by introducing crease hinges along the ruling lines of the surface.

Developable mechanisms are mechanisms that "conform to developable surfaces when both are modeled with zero thickness" [9]. This zero-thickness surface is called the developable mechanism's reference surface [5]. The links of a developable mechanism should not be required to deform in order for the mechanism to have motion. This can be achieved by aligning hinge lines with the reference surface's ruling lines [9]. In at least one position, the conformed position, the mechanism's links must conform to the developable reference surface. This requires the rigid links to be shaped to the surface when in their conformed position [5]. Cylindrical developable mechanisms have been discussed by [5] and have inspired the creation of surgical devices [12]. Since the beginning of this work, additional work has been done on conical developable mechanisms which is presented in [6].

The motivation of this paper is the demonstration of the mathematical modeling and analysis of developable mechanisms that can be constructed using kirigami techniques, similar to designs for planar surfaces. Kirigami is a variation of origami that includes cutting in addition to folding [11]. Kirigami has inspired the creation of lamina emergent mechanisms, or mechanisms that can be fabricated in a plane, and then emerge from the surface [7]. Both planar and spherical lamina emergent mechanisms are possible [16]. Although originally based on planar surfaces, lamina emergent mechanisms have facilitated the creation of deployable mechanisms on other developable surfaces, such as cylinders and cones [10]. The *lamina emergent planar*

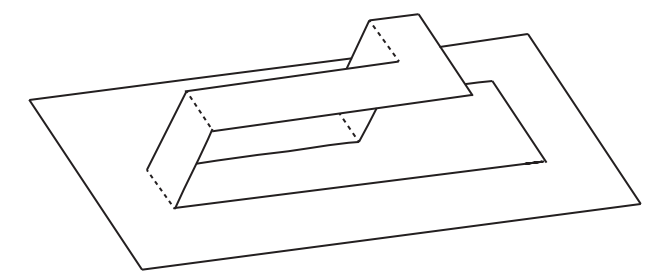


FIGURE 1: A lamina emergent planar mechanism that has rigid motion

mechanism shown in Figure 1 is a developable mechanism that is constructed from a planar surface using kirigami and consists of panels linked at hinge joints whose hinge lines are all parallel. This mechanism has parallelogram linkage and therefore is a special case Grashof mechanism. As a result, the mechanism illustrated will have *change points*, which correspond to bifurcation points in its motion paths.

In this paper, we construct an analogous mechanism cut out of a cone as shown in Figure 2. This mechanism employs the principles of both developable mechanisms and lamina-emergent mechanisms and will be referred to as a *developable conical mechanism* because it is constructed from a cone. Note that the particular developable conical mechanism also has parallelogram linkage. Thus, if a rigid motion exists, it will necessarily have change points. We will proceed by providing a model of the the motion of the mechanism, and then prove analytically that a rigid motion, or motion without deforming the surface or the links, does exist. We will then provide a detailed description of it motion, with special attention to the initial motion from its conformed position at bifurcation points in the motion path.

2 Construction and Setup

In this section, we detail the construction of the developable conical mechanism and begin to set up the mathematical model utilized in determining the rigid motion of the panels on the mechanism.

2.1 The Mechanism

Let $\mathcal{C} \subset \mathbb{R}^3$ be a cone centered on the positive *z*-axis with its cone point at the origin, and having cone angle ϕ . The developable conical mechanism is constructed by cutting out a section of the cone and folding along hinge lines to form three panels (links) with the remainder of the cone forming a fourth panel (link), as shown in Figure 2. The panel P_0 is the main body of the cone. The panels P_1 and P_2 are joined to the body of the cone along hinge lines, which we will call H_1 and H_2 , respectively. Panel P_3 emerges out of the cone and is connected to panels P_1

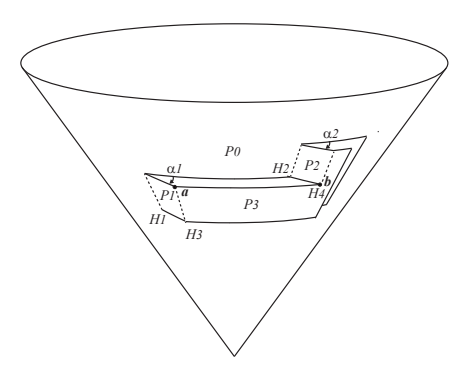


FIGURE 2: The developable conical mechanism. Panels P_i , hinges H_i , and motion parameters α_i are indicated.

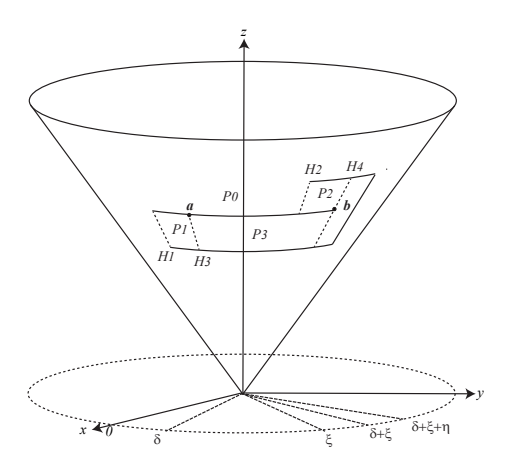


FIGURE 3: The design of the developable conical mechanism in the conformed position.

and P_2 along hinge lines, which we will call H_3 and H_4 , respectively.

Choose angles $\delta, \xi \in (0, 2\pi)$ so that $\delta + \xi < 2\pi$. Also choose positive numbers z_1, z_2 , and z_3 with $z_1 < z_2 < z_3$. Considering \mathbb{R}^3 with cylindrical coordinates (see Figure 3), the panels P_1 and P_2 are defined by:

$$P_1 = \{ (r, \theta, z) \in \mathcal{C} : z_1 < z < z_2, \ 0 < \theta < \delta \},$$

$$P_2 = \{ (r, \theta, z) \in \mathcal{C} : z_2 < z < z_3, \ \xi < \theta < \delta + \xi \}.$$

Note that we can also choose an $\eta > 0$ so that $\delta + \xi + \eta < 2\pi$. The third panel, panel P_3 , which joins P_1 and P_2 is given by:

$$P_{3} = \{(r, \theta, z) \in \mathscr{C} : z_{1} < z < z_{2}, \delta < \theta < \delta + \xi + \eta\}$$

$$\cup \{(r, \theta, z) \in \mathscr{C} : z_{2} < z < z_{3}, \ \delta + \xi < \theta < \delta + \xi + \eta\}.$$

Viewing the main body of the cone P_0 as fixed, the panels P_1 and P_2 will rotate rigidly about their respective hinge lines H_1 and H_2 . The angle from which the panel P_1 rotates about hinge line H_1 is denoted α_1 , with $\alpha_1 = 0$ corresponding to P_1 being in the conformed position (i.e., being flush with the body of the cone). Similarly, the angle from which the panel P_2 rotates about the hinge line H_2 is denoted α_2 , with $\alpha_2 = 0$ corresponding to P_2 being in the conformed position. We define the positive direction of the angle to correspond to an initial outward movement. We desire to find a relationship between α_1 and α_2 so that we can ensure that the rigid motion of panels P_1 and P_2 will admit a rigid motion for P_3 so that P_3 remains joined to P_1 and P_2 along the hinge lines H_3 and H_4 .

Because the position of panel P_1 in \mathbb{R}^3 depends on α_1 , we refer to the image of P_1 in \mathbb{R}^3 resulting from a rotation of α_1 as $P_1[\alpha_1]$. The image of P_2 resulting from a rotation of α_2 is denoted as $P_2[\alpha_2]$. Similarly, the image of the hinge lines H_3 and H_4 in \mathbb{R}^3 , with respect to the angles on which they depend, will be denoted $H_3[\alpha_1]$ and $H_4[\alpha_2]$, respectively.

We can now clearly see that the developable conical mechanism is a spherical mechanism. A *spherical mechanism* consists of bars linked at hinge joints whose hinge lines all intersect at a point. The conical reference surface has ruling lines that meet at the cone point (or apex of the cone). Because it is necessary for the mechanism's hinge lines to be constructed along the ruling lines of the cone, in order to obtain motion without deformation, and throughout the motion the hinge lines continue to meet at the cone point, the mechanism must be a spherical mechanism centered about the cone point (See also [6]).

2.2 Defining Points

Consider the following two points on the undeflected mechanism given in cylindrical coordinates:

$$\mathbf{a} = [z_2 \tan \phi, \delta, z_2],$$

$$\mathbf{b} = [z_2 \tan \phi, \delta + \xi, z_2].$$

Note that these two points lie on the hinge lines $H_3[0]$ and $H_4[0]$. Indeed, we will be interested in the points **a** and **b** as they rotate with the panels $P_1[\alpha_1]$ and $P_2[\alpha_2]$. We denote these rotated points by $\mathbf{a}[\alpha_1]$ and $\mathbf{b}[\alpha_2]$, respectively.

Converting to Cartesian coordinates, the points $\mathbf{a}[0]$ and $\mathbf{b}[0]$ are:

$$\mathbf{a} = \langle z_2 \tan \phi \cos \delta, z_2 \tan \phi \sin \delta, z_2 \rangle, \tag{1}$$

$$\mathbf{b} = \langle z_2 \tan \phi \cos(\delta + \xi), z_2 \tan \phi \sin(\delta + \xi), z_2 \rangle. \tag{2}$$

2.3 Motion via Linear Transformation

The motion of a panel about a hinge line H_i for i = 1, 2 can be described through a series of linear transformations. The com-

position of the following transformations will provide the transformations that describe the motion of panel P_i so that we can determine $P_i[\alpha_1]$:

I. The first transformation moves hinge line H_i to the xz-plane by a clockwise rotation by an angle ω about the z-axis:

$$A_0(\omega) = \begin{pmatrix} \cos \omega & \sin \omega & 0 \\ -\sin \omega & \cos \omega & 0 \\ 0 & 0 & 1 \end{pmatrix}. \tag{3}$$

II. Next, we move the image of hinge line H_i to the z-axis by a clockwise rotation of the cone angle ϕ about the y-axis:

$$A_1(\phi) = \begin{pmatrix} \cos \phi & 0 - \sin \phi \\ 0 & 1 & 0 \\ \sin \phi & 0 & \cos \phi \end{pmatrix}. \tag{4}$$

III. This next rotation about the z-axis by an angle α_i is the key transformation. Having applied the transformations $A_0(\omega)$ and $A_1(\phi)$, the image of the hinge line H_i now lies on the z-axis. Hence, the rotation of panel P_i about the hinge line H_i at this step is realized by:

$$A_2(\alpha_i) = \begin{pmatrix} \cos \alpha_i & \sin \alpha_i & 0 \\ -\sin \alpha_i & \cos \alpha_i & 0 \\ 0 & 0 & 1 \end{pmatrix}.$$
 (5)

IV. The transformation $A_1(-\phi)$ reverses the action of $A_1(\phi)$:

$$A_1(-\phi) = \begin{pmatrix} \cos\phi & 0 & \sin\phi \\ 0 & 1 & 0 \\ -\sin\phi & 0 & \cos\phi \end{pmatrix}. \tag{6}$$

V. Finally, the transformation $A_0(-\omega)$ reverses the action of $A_0(\omega)$:

$$A_0(-\omega) = \begin{pmatrix} \cos \omega - \sin \omega & 0\\ \sin \omega & \cos \omega & 0\\ 0 & 0 & 1 \end{pmatrix}. \tag{7}$$

We assume that the cone is initially positioned so that $\omega = 0$ for H_1 and $\omega = \xi$ for H_2 (i.e. the mechanism is in its conformed position). Composing these transformations, we define:

$$T_1(\alpha_1) = A_0(0)A_1(-\phi)A_2(\alpha_1)A_1(\phi)A_0(0),$$
 (8)

$$T_2(\alpha_2) = A_0(-\xi)A_1(-\phi)A_2(\alpha_2)A_1(\phi)A_0(\xi). \tag{9}$$

Notice that in the definitions of $T_1(\alpha_1)$ and $T_2(\alpha_2)$, we chose the arguments of A_0 to coincide with the azimuth angle of the hinge lines H_1 and H_2 in cylindrical coordinates. Therefore, $T_i(\alpha_i)$ applied to any point has the effect of rotating that point about the hinge line H_i for i=1,2. Thus, it is simple to define the motion of the panels P_1 and P_2 about their hinge lines:

$$P_1[\alpha_1] = T_1(\alpha_1)P_1[0],$$

 $P_2[\alpha_2] = T_2(\alpha_2)P_2[0].$

Since $\mathbf{a}[\alpha_1]$ if a point of $P_1[\alpha_1]$ and $\mathbf{b}[\alpha_2]$ is a point of $P_2[\alpha_2]$ we can write:

$$\mathbf{a}[\alpha_1] = T_1(\alpha_1)\mathbf{a}[0], \tag{10}$$

$$\mathbf{b}[\alpha_2] = T_2(\alpha_2)\mathbf{b}[0]. \tag{11}$$

3 Rigid Motion

For the developable conical mechanism to have rigid motion, panels P_1 and P_2 must move by a rotation about their hinge lines H_1 and H_2 , respectively. Our goal is to find an open interval U of the real line containing 0 and a function $f: U \to \mathbb{R}$ so that the rigid motion of panels P_1 and P_2 given by $P_1[\alpha_1]$ and $P_2[f(\alpha_1)]$ admits a rigid motion for P_3 as well.

Supposing that such a function f exists, a necessary condition for a rigid motion on panel P_3 is that the distance between points $\mathbf{a}[\alpha_1]$ and $\mathbf{b}[f(\alpha_1)]$ remains constant as α_1 varies. In fact, as we shall see from the Rigidity Theorem in the next section, this condition is both necessary and sufficient.

Our strategy, therefore, will be to examine the level sets of the function $D: \mathbb{R}^2 \to \mathbb{R}$ defined by:

$$D(\alpha_1, \alpha_2) = \|\mathbf{a}[\alpha_1] - \mathbf{b}[\alpha_2]\|^2 \tag{12}$$

where $\mathbf{a}[\alpha_1]$ and $\mathbf{b}[\alpha_2]$ are given by Equations 10 and 11, which reference Equations 1, 2, 8, 9, and then Equations 1 - 7. Then D represents the square of the standard Euclidean norm between $\mathbf{a}[\alpha_1]$ and $\mathbf{b}[\alpha_2]$.

Note that $D(\alpha_1,\alpha_2)$ is dependent on the design parameters ϕ , δ , ξ and z_2 . However, it is sufficient for our analysis to set $z_2=1$. This is the case because although z_2 modifies the magnitude of the function D, it does not effect the D(0,0)-level set, which determines possible motion paths. In other words, the movement of two mechanism with the same design parameter, except the z_i values (i=1,2,3), is exactly the same.

We will find that variations of the design parameters ϕ , δ , and ξ do change the D(0,0)-level set and may significantly modify the general behavior of the mechanism. When needed to facilitate the discussion of the analysis of the function, we extend

the notation of $D(\alpha_1, \alpha_2)$ to

$$D[\phi, \delta, \xi](\alpha_1, \alpha_2).$$

When we use the notation $D(\alpha_1, \alpha_2)$, we assume the values for ϕ , δ and ξ are given.

The reader may note that the explicit formulas for Equations 8 - 12 become quite lengthy and challenging to analyze. Thus we first verify the existence of a rigid motion by a theoretical analysis. We then demonstrate how to evaluate a rigid motion path computationally.

3.1 Existence of a Rigid Motion

First, we will prove that there exists an open interval U of the real line containing 0 and a function $f:U\to\mathbb{R}$ so that f(0)=0 and $D(\alpha_1,f(\alpha_1))$ is constant. The reasoning here is quite easy, as we will appeal to the Implicit Function Theorem. The explicit form of $D(\alpha_1,\alpha_2)$ is lengthy, but the gradient at the origin is given by:

$$\nabla D(0,0) = \begin{pmatrix} 8z_2^2\sin\frac{\xi}{2}\sin\phi\tan\phi\sin\frac{\delta}{2}\sin(\frac{\delta+\xi}{2}) \\ 4z_2^2\sin\frac{\xi}{2}\sin\phi\tan\phi\left(\cos(\delta+\frac{\xi}{2})-\cos(\frac{\xi}{2})\right) \end{pmatrix}.$$

To apply the Implicit Function Theorem, we must guarantee that $\nabla D(0,0) \neq (0,0)$. Both components of $\nabla D(0,0)$ are a product of several factors. We will simply show that all factors are nonzero.

 $z_2 \neq 0$ because we chose it to be positive. Since $0 < \xi < 2\pi$, we have $\sin \frac{\xi}{2} \neq 0$. Since $0 < \phi < \pi/2$, we have $\sin \phi \neq 0$ and $\tan \phi \neq 0$. Showing that

$$\cos\left(\delta + \frac{\xi}{2}\right) - \cos\frac{\xi}{2} \neq 0$$

requires some work. We will prove by contradiction. Supposing that equality holds and applying the angle addition formula for cosine gives us

$$\cos\delta\cos\frac{\xi}{2} - \sin\delta\sin\frac{\xi}{2} - \cos\frac{\xi}{2} = 0.$$

Rearranging terms gives us

$$\frac{\cos\delta - 1}{\sin\delta} = \tan\frac{\xi}{2}.$$

Applying the half angle identity for tangent, we are left with

$$\tan\left(-\frac{\delta}{2}\right) = \tan\frac{\xi}{2}.$$

This means that $\frac{\delta}{2} + \frac{\xi}{2} = n\pi$ for some integer n, or

$$\xi + \delta = 2n\pi$$
.

But we have chosen ξ and δ so that $0 < \xi + \delta < 2\pi$. So this is a contradiction. Thus,

$$\cos\left(\delta + \frac{\xi}{2}\right) - \cos\frac{\xi}{2} \neq 0.$$

Since none of the factors in the first component of $\nabla D(0,0)$ are equal to zero,

$$\nabla D(0,0) \neq (0,0).$$

The Implicit Function Theorem tells us that there is an open interval $U \subset \mathbb{R}$ containing 0 and a function $f: U \to \mathbb{R}$ so that f(0) = 0 and $D(\alpha_1, f(\alpha_1))$ is constant for all $\alpha_1 \in U$. We can now conclude that there exists some rigid motion of the mechanism.

3.2 Solving for the Motion Path

Because of its non-constructive nature, the Implicit Function Theorem does not specify the rigid motion. However, the rigid motion can be described by a level set that is determined explicitly as the solution to a differential equation. For the purposes of setting up and solving this differential equation, we will write both α_1 and α_2 as functions of another parameter t, and use the function $\mathbf{r}: \mathbb{R} \to \mathbb{R}^2$ defined by:

$$\mathbf{r}(t) = (\alpha_1(t), \alpha_2(t)).$$

The differential equation whose solution traces out the level curve is the so-called *gradient equation*. It is given by:

$$\nabla D(\alpha_1, \alpha_2) \cdot \mathbf{r}'(t) = 0,$$

with the initial value

$$\mathbf{r}(0) = (0,0).$$

This is a nonlinear ordinary differential equation which is underdetermined because we have just one equation with two unknown functions, $\alpha_1(t)$ and $\alpha_2(t)$. We can remedy this by setting:

$$\alpha_1(t) = t$$
.

Thus, we are left to solve:

$$D_{\alpha_1}(t,\alpha_2(t)) + D_{\alpha_2}(t,\alpha_2(t))\alpha_2'(t) = 0$$

or

$$\alpha_2'(t) = -\frac{D_{\alpha_1}(t, \alpha_2(t))}{D_{\alpha_2}(t, \alpha_2(t))}.$$
(13)

Equation 13 can be expanded by referencing Equation 12, substituting in the explicit forms of equations 10 and 11, and taking the appropriate partial derivatives. However, the expanded form is quite lengthy, so we leave it in symbolic form.

We illustrate graphs of the $D(\alpha_1, \alpha_2)$ for several variations of the design parameters δ , ξ , and ψ in Figures 4 and 5. Note that D(0,0) is the functional value of D when the conical mechanism is in its conformed position. The curves indicated within the graphs are the D(0,0)-level curves (i.e. the set of points for which $D(\alpha_1,\alpha_2)=D(0,0)$) and are obtained by numerically solving the differential equation, Equation 13, for $\alpha_2(t)$ and then plotting the collection of points $(t,\alpha_2(t))$.

As illustrated in Figure 6, there are multiple possible paths that are connected to the origin. In the next section, we verify that these parameter functions are sufficient to define a rigid motion. It is clear that the relationship between the parameter functions α_1 and α_2 is necessary. To see an animation of how panels move on these paths, refer to the following link: https://www.youtube.com/watch?v=pydi04PRjDw.

3.3 Observational Analysis

Considering Figure 6, note that in all cases there is a class of upward slanting curves which represent motion in which α_1 and α_2 are increasing at nearly the same rate. We will refer to these curves as the \mathscr{E} -curves. The other curves we will refer to as the \mathscr{D} -curves. Note that the origin is contained in a \mathscr{D} -curve in each case.

The points where two motion curves intersect are called *bifurcation points*, and correspond to the change points of the mechanism. A bifurcation point represents a point in the motion in which there is more that one possible continuation of the motion, other than reversing the motion. For planar lamina emergent mechanisms, there must be a bifurcation point corresponding to when the mechanism is in its conformed position [7]. However,

for this developable conical mechanism, such is not the case. The conformed position generally does not correspond to a bifurcation point, as illustrated in Figure 6. Indeed, when $\delta \neq \xi$, the bifurcation points occur when the hinge lines lie in a single plane (see [10]), which is not the case in the conformed position. However, suppose $\delta = \xi$. In the case that $\alpha_1 = \alpha_2 = 0$ (the conformed position), we note that H_2 and H_3 are colinear and P_2 and P_3 can rotate freely about this axis while holding P_1 fixed. Likewise, in the case that $\alpha_1 = \alpha_2 = \pi$, we note that H_1 and H_4 are colinear and P_1 and P_3 can rotate freely about this axis while holding P_2 fixed.

When $\delta \neq \xi$, the bifurcation points arise only from the intersection of $\mathscr E$ -curves with $\mathscr D$ -curves. However, when $\delta = \xi$ bifurcation points may also arise from the intersection of $\mathscr D$ -curves. We will refer to a bifurcation point that is the intersection of an $\mathscr E$ -curve with a $\mathscr D$ -curve as an *ordinary bifurcation point* and a bifurcation point that is the intersection of two $\mathscr D$ -curves as an *extraordinary bifurcation point*. At ordinary bifurcation points, the hinge lines are coplanar but not colinear. At extraordinary bifurcation points, the hinge lines are coplanar and a pair of hinge lines, H_2 and H_3 or H_1 and H_4 , is colinear.

To understand the transition of the shapes of the \mathscr{D} -curves as δ changes size in comparison to ξ , note that when $\delta=\xi$, the \mathscr{D} -curves can be represented as a set of vertical and horizontal lines. Thus the region of space near an extraordinary bifurcation point is divided into four quadrants. When δ decreases away from ξ , the \mathscr{D} -curves break into two continuous curves: one in the first quadrant and one in the third quadrant. Likewise, when δ increases away from ξ , the \mathscr{D} -curves break into two continuous curves: one in the second quadrant and one in the fourth quadrant.

3.3.1 Initial Motion The compact nature of the developable conical mechanism is achieved when the mechanism is in its conformed position. As such it is important to consider the initial motion of the mechanism, or the motion as the mechanism moves from the conformed position. Greenwood described three behaviors (intramobility, extramobility, and transmobility) that characterize the motion of developable mechanisms as they move from their conformed position. Graphical methods exist for predicting these behaviors for regular cylindrical [5] and conical [6] developable mechanisms. We also note that as a change point mechanisms there are two possible configurations, open and crossed, and that the conformed position represents a crossed configuration (see [7]).

We provide an analytical perspective for regular conical developable mechanisms. Note that if all panels start in the conformed position, the initial motion must be defined by a path that moves along a \mathscr{D} -curve. The initial direction of the \mathscr{D} -curve depends on the relative sizes of δ and ξ , as follows:

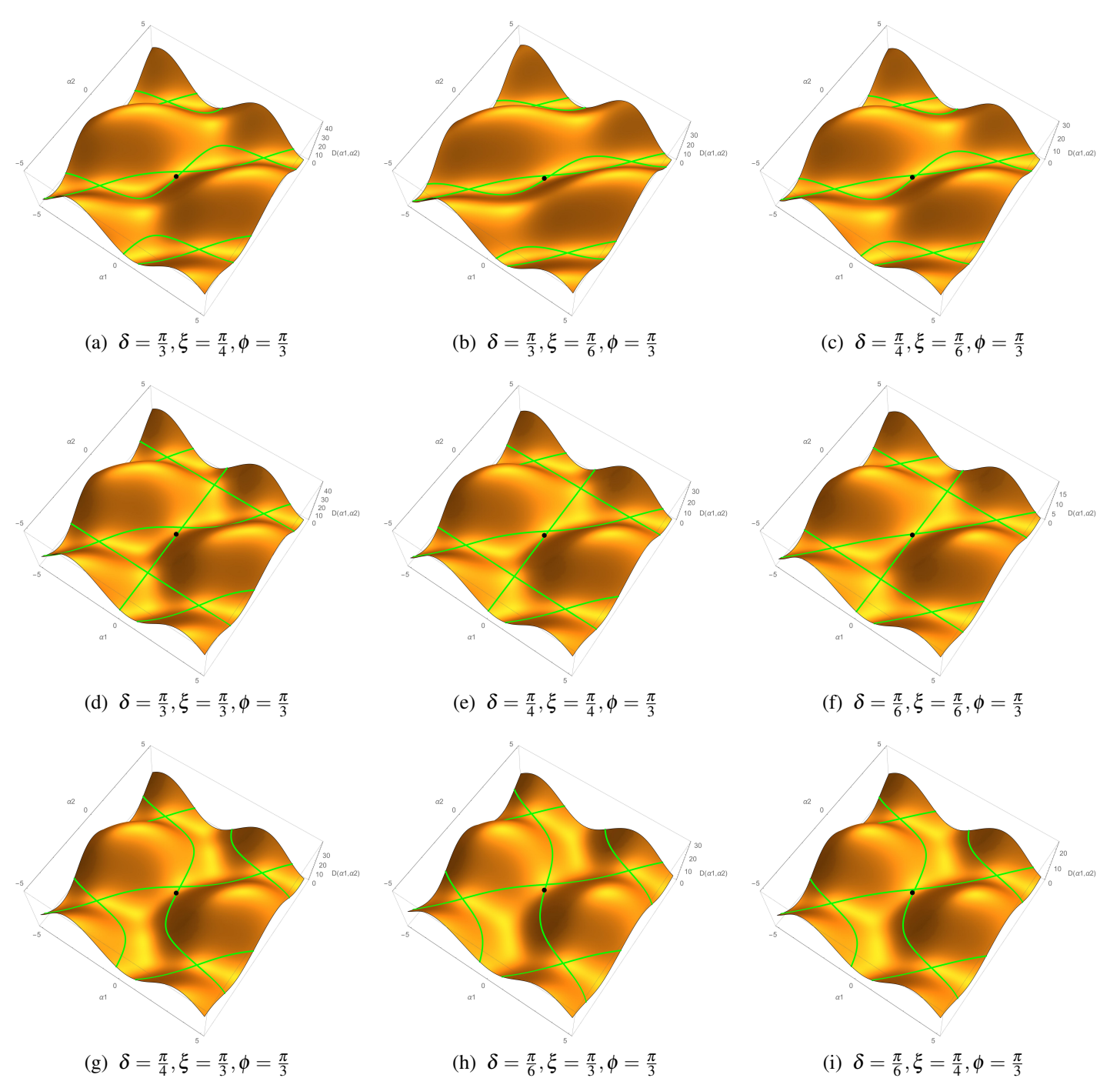


FIGURE 4: Plots of the function $D(\alpha_1, \alpha_2)$ for $\phi = \frac{\pi}{3}$ and differing δ and ξ values. The level curves $D(\alpha_1, \alpha_2) = D(0, 0)$ are also indicated.

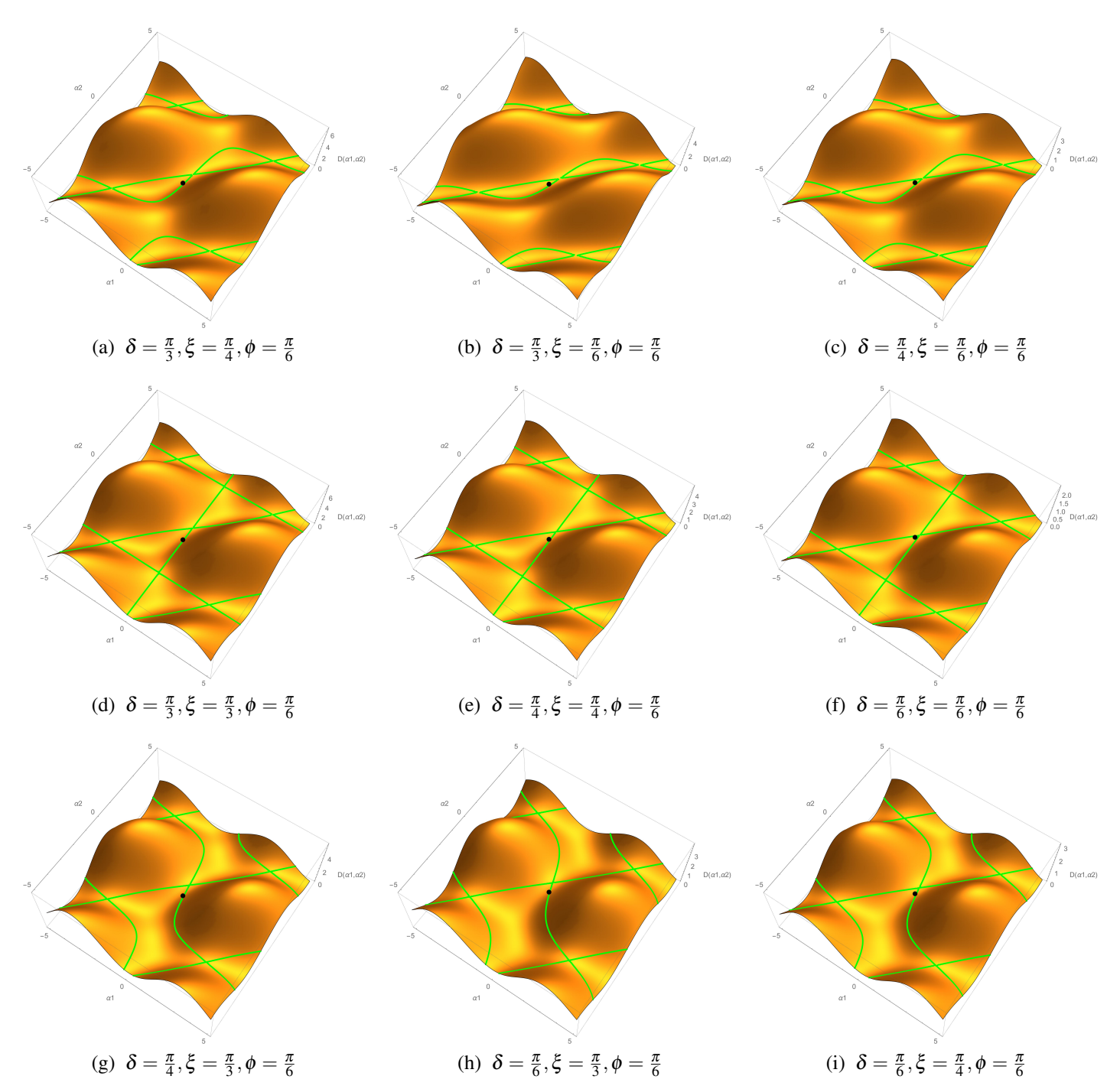


FIGURE 5: Plots of the function $D(\alpha_1, \alpha_2)$ for $\phi = \frac{\pi}{6}$ and differing δ and ξ values. The level curves $D(\alpha_1, \alpha_2) = D(0, 0)$ are also indicated.

If $\delta < \xi$, we observe that when α_1 is initially increasing, then α_2 is initially increasing (see Figure 6A). Hence, if panel P_1 is initially moving outward, then panel P_2 must be initially moving inward, and vice versa. Greenwood et. al. [5] refers to this type of behavior as *transmobile*.

If $\delta = \xi$, recall that this is the case where H_2 and H_3 are colinear in the conformed position. Thus, panel P_1 must initially be kept fixed while panel P_2 moves in either direction (see Figure 6B).

If $\delta > \xi$, we observe that both panels initially move in the same direction, but P_1 moves at a slower rate than P_2 (see Figure 6C). This behavior is called *intramobile* if the motion is towards the interior of the surface and *extramobile* if the motion is towards the exterior of the surface [5].

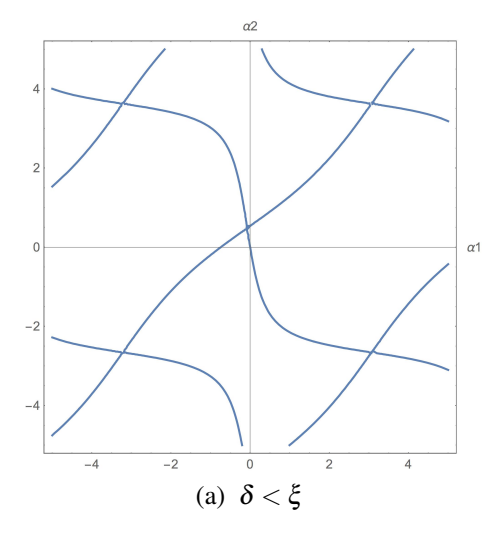
3.3.2 Bifurcation Points The characteristics of the possible continued motions at a bifurcation point also depend on the relative sizes of δ and ξ . At a bifurcation point:

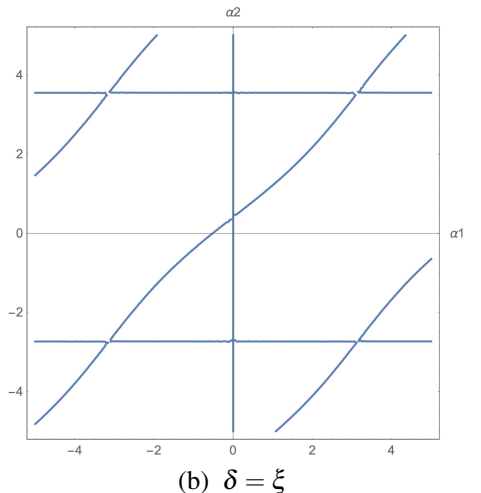
If $\delta < \xi$, we observe that it is possible to move panels P_1 and P_2 in the same direction by continuing the motion along an \mathscr{E} -curve, or in a different direction by continuing the motion along a \mathscr{D} -curve. In this case, all bifurcation points are ordinary. The set of bifurcation points connected to the origin is periodic in one direction. There are an infinite number of parallel sets.

If $\delta = \xi$, we observe that at an ordinary bifurcation point there is a choice to keep one panel, P_1 or P_2 , fixed while moving the other, or to keep both panels in motion at nearly the same rate. At an extraordinary bifurcation point, only one panel can be put in motion while fixing the other, but either panel can be selected to be put in motion. In this case, all bifurcation points are connected to the origin. Both the set of ordinary bifurcation points and the set of extraordinary bifurcation points each form an array that is periodic in two directions.

If $\delta > \xi$, we observe that both panels P_1 and P_2 must continue to move in the same direction. However, there are two possible rates at which this occurs. In this case, all bifurcation points are ordinary and connected to the origin. They form an array that is periodic in two directions.

The existence of the bifurcation points lead to unbounded motion paths in the $\alpha_1\alpha_2$ -plane. When $\delta < \xi$, the bifurcation points are periodic in two directions and all bifurcation points are connected to the origin. Each $\mathscr E$ -curve intersects each $\mathscr D$ -curve at precisely one point. When $\delta > \xi$, the bifurcation points form parallel sets with an infinite number of points in each set. The parallel sets consist of the intersection points of a single $\mathscr E$ -curve





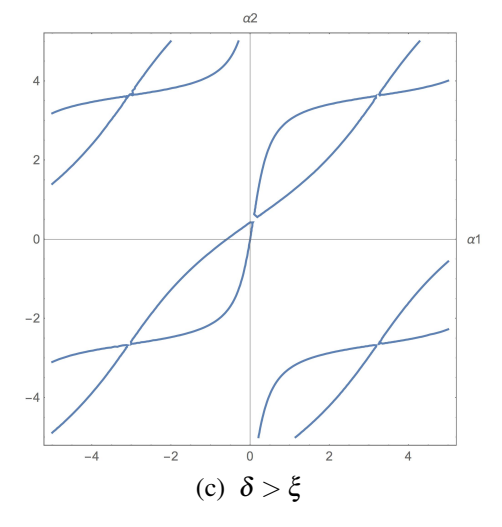


FIGURE 6: The characteristics of the paths of motion depending on the relative sizes of ξ and δ .

with a single \mathscr{D} -curve. Only one parallel set of bifurcation points contain points connected to the origin. There is a one-to-one correspondence between the \mathscr{E} -curves and \mathscr{D} -curves that intersect.

Note that, by design, our developable conical mechanism is a parallelogram linkage, a special-case Grashof mechanism. For modifications of our design that do not result in parallelogram linkage, see [6]. For these more generally designed mechanisms, the existence and types of bifurcation points in the motion will depend on whether or not they are Grashof mechanisms.

4 The Rigid Transformation

In this section, we define the rigid motion that acts on the developable conical four-bar mechanism. The rigid motion $T: \mathbb{R}^3 \times \mathbb{R} \to \mathbb{R}^3$ is piecewise defined as follows:

Recall that $T_1(t)$, $T_2(t)$, **a**, and **b** were defined in Section 2 by Equations 1, 2, 8, 9. We define T to be:

$$T(t)\mathbf{x} = \begin{cases} \mathbf{x}, & \text{if } \mathbf{x} \in P_0 \\ T_1^*(t)\mathbf{x}, & \text{if } \mathbf{x} \in P_1 \\ T_2^*(t)\mathbf{x}, & \text{if } \mathbf{x} \in P_2 \\ T_3^*(t)\mathbf{x}, & \text{if } \mathbf{x} \in P_3 \end{cases}$$
(14)

where

$$T_1^*(t) = T_1(t)$$
 and $T_2^*(t) = T_2(\alpha(t))$.

To define $T_3^*(t)$, let $\mathbf{c} = \mathbf{a} \times \mathbf{b}$. Note that $\{\mathbf{a}, \mathbf{b}, \mathbf{c}\}$ form a basis for \mathbb{R}^3 . Then each point $\mathbf{x} \in \mathbb{R}^3$ can be written as:

$$\mathbf{x} = k_a \mathbf{a} + k_b \mathbf{b} + k_c \mathbf{c}$$

where k_a , k_b , and k_c are a unique set of constants. We define $T_3^*(t): \mathbb{R}^3 \to \mathbb{R}^3$ by

$$T_3^*(t)\mathbf{x} = k_a T_1^*(t)\mathbf{a} + k_b T_2^*(t)\mathbf{b} + k_c [T_1^*(t)\mathbf{a} \times T_2^*(t)\mathbf{b}].$$

Theorem 1. T(t) defines a rigid motion.

Proof. To see that T(t) is well-defined, first note that by construction $T_1^*(t)$ and $T_2^*(t)$ are the identity on hinge lines H_1 and H_2 , respectively. Thus, the mapping T(t) is well-defined on the points of P_0 intersecting P_1 or P_2 . Next, we need to verify that $T_3^*(t)$ is consistent with $T_1^*(t)$ and $T_2^*(t)$ on hinge lines H_3 and H_4 , respectively. Note that:

1. If $\mathbf{x} \in H_3$, then $\mathbf{x} = k_a \mathbf{a}$. Thus $T_3^*(t) \mathbf{x} = k_a T_1^*(t) \mathbf{a} = T_1^*(t)(k_a \mathbf{a}) = T_1^*(t) \mathbf{x}$. Hence

$$T_3^*(t)\mathbf{x} = T_1^*(t)\mathbf{x}.$$

2. If $\mathbf{x} \in H_2$, then $\mathbf{x} = k_b \mathbf{b}$. Thus $T_3^*(t)\mathbf{x} = k_b T_2^*(t)\mathbf{b} = T_2^*(t)(k_b \mathbf{b}) = T_2^*(t)\mathbf{x}$. Hence

$$T_3^*(t)\mathbf{x} = T_2^*(t)\mathbf{x}.$$

Thus we have the desired result. Therefore T(t) is well-defined. It is now clear from the definition of $T_3^*(t)$ and using the substitutions

$$T_3^*(t)\mathbf{a} = T_1^*(t)\mathbf{a}$$

 $T_3^*(t)\mathbf{b} = T_2(t)\mathbf{b}$
 $T_3^*(t)\mathbf{c} = T_1^*(t)\mathbf{a} \times T_2^*(t)\mathbf{b}$,

that for $\mathbf{x} = k_a \mathbf{a} + k_b \mathbf{b} + k_c \mathbf{c} \in \mathbb{R}^3$,

$$T_3^*(t)\mathbf{x} = k_a T_3^*(t)\mathbf{a} + k_b T_3^*(t)\mathbf{b} + k_c T_3^*(t)\mathbf{c}.$$
 (15)

Using the identity given in Equation 15, the fact that T_3^* is a linear transformation is a straightforward verification. In particular, for constants λ_1 and λ_2 and vectors

$$\mathbf{x_1} = k_{a_1} \mathbf{a} + k_{b_1} \mathbf{b} + k_{c_1} \mathbf{c}$$

 $\mathbf{x_2} = k_{a_2} \mathbf{a} + k_{b_2} \mathbf{b} + k_{c_2} \mathbf{c}$

we can immediately verify that

$$T_3^*(t)(\lambda_1\mathbf{x_1} + \lambda_2\mathbf{x_2}) = \lambda_1T_3^*(t)\mathbf{x_1} + \lambda_2T_3^*(t)\mathbf{x_2}.$$

By construction, $T_1^*(t)$ and $T_2^*(t)$ are orthogonal transformations. To see that $T_3^*(t)$ is an orthogonal transformation, note that by design, the distance between $T_1^*(t)\mathbf{a}$ and $T_2^*(t)\mathbf{b}$ remains constant as t varies. Thus, for all t, the triangle with vertices $\mathbf{0}$, \mathbf{a} , and \mathbf{b} is congruent to the triangle with vertices $T(t)\mathbf{0}$, $T(t)\mathbf{a}$, and $T(t)\mathbf{b}$. Hence, $T_3^*(t)\mathbf{c} = T_1^*(t)\mathbf{a} \times T_2^*(t)\mathbf{b}$ has constant magnitude and is perpendicular to both $T_1^*(t)\mathbf{a}$ and $T_2^*(t)\mathbf{b}$ throughout the motion. This means the tetrahedron with vertices $\mathbf{0}$, \mathbf{a} , \mathbf{b} , and \mathbf{c} is congruent to the tetrahedron with vertices $T_3^*(t)\mathbf{0}$, $T_3^*(t)\mathbf{a}$, $T_3^*(t)\mathbf{b}$, and $T_3^*(t)\mathbf{c}$. Thus, it must be the case that $T_3^*(t)$ is an orthogonal transformation. Therefore T(t) defines a rigid motion.

Note that the argument above does not depend on $\mathscr C$ being a circular cone, nor that $\mathbf a$ and $\mathbf b$ have the same z-coordinate. It is only required that $T_1^*(t)$ and $T_2^*(t)$ are orthogonal transforms and that the distance between $T_1^*(t)\mathbf a$ and $T_2^*(t)\mathbf b$ is constant throughout the motion. Thus, we can summarize these results by the following theorem.

Theorem 2. Suppose C is a generalized cone in \mathbb{R}^3 with cone point at $\mathbf{0}$ and a developable conical mechanism is constructed on C, similarly as in Figure 2, with hinge lines H_1 , H_2 , H_3 , and H_4 passing through the origin. Let \mathbf{a} and \mathbf{b} be points distinct from the origin on the hinge lines H_3 and H_4 , respectively. If there are linear transformation paths $T_1^*(t)$ and $T_2^*(t)$ acting on panels P_1 and P_2 , respectively, so that the distance between $T_1^*(t)\mathbf{a}$ and $T_2^*(t)\mathbf{b}$ are constant as t varies, then the motion defined by (14) is a rigid motion.

5 Conclusion

In this paper we have demonstrated that developable conical mechanisms, as designed here, have rigid motion. We have also demonstrated how to analytically determine that motion and have provided general descriptions of the motion. The relationship between variables δ and ξ determines the motion of the mechanism with respect to the conical reference surface and predicts the behaviors (intramobile, extramobile, transmobile) the mechanism can exhibit. Furthermore, we proved that a conical four-bar mechanism constructed on a generalized cone has rigid motion provided that a motion can be found that preserves the distance between any two distinct points, one on each of hinge lines H_3 and H_4 .

Acknowledgment

This research was done under grant No. 1663345 from the National Science Foundation.

References

- [1] Ceccato, C., 2012, Material Articulation: Computing and Constructing Continuous Differentiation. Architectural Design. **82** (2), 96.
- [2] Decaudin, P., Julius, D., Wither, J., Boissieux, L., Sheffer, A., and Cani, M., 2006, Virtual Garments: A Fully Geometric Approach for Clothing Design. Computer Graphics Forum, 25 (3), 625.
- [3] Farmer, R. S., 1938, Celestial Cartography. Publications of the Astronomical Society of the Pacific **50** (293), 34-48.
- [4] Fuchs, D., and Tabachnikiov, S., 1999, More on Paper Folding. The American Mathematical Monthly, **106** (1), 27-35.
- [5] Greenwood, J. R., Magleby, S. P., and Howell L. L., 2019, Developable mechanisms on regular cylindrical surfaces. Mechanism and Machine Theory, 142, 103584. doi.org/10.1016/j.mechmachtheory.2019.103584
- [6] Hyatt, L. P., Magleby, S. P., and Howell L. L., 2020, Developable mechanisms on right conical surfaces, Mechanism and Machine Theory, 149, 103813. doi.org/10.1016/j.mechmachtheory.2020.103813, 2020.

- [7] Jacobsen, J. O., Winder, B. G., Howell, L. L., and Magleby, S. P., 2009, Lamina Emergent Mechanisms and Their Basic Elements. ASME. J. Mechanisms Robotics, February 2010, 2 (1) 011003. doi.org/10.1115/1.4000523
- [8] Perez, F. and Suarez, J. A., 2007, Quasi-developable B-spline surfaces in ship hull design. Computer Aided Design, **39** (10), 853 862.
- [9] Nelson, T., Zimmerman, T., Magleby, S., Lang, R., and Howell, L., 2019, Developable Mechanisms on Developable Surfaces. Science Robotics, 4 (2). doi: 10.1126/scirobotics.aau5171
- [10] Nelson, T. G., Lang, R. J., Pehrson, N. A., Magleby, S. P., and Howell, L. L., 2016, Facilitating Deployable Mechanisms and Structures Via Developable Lamina Emergent Arrays. Journal of Mechanisms and Robotics, 8 (3), 031006-(1-10).
- [11] Shyu, T. C., Damasceno, P. F., Dodd, P. M., Lamboureux, A., Xu, L., Shlian, M., Shtein, M., Glotzer, S. C., and Kotov, N. A., 2015, A kirigami approach to engineering elasticity in nanocomposites through patterned defects. Nature Materials 14, 785-789. doi:10.1038/nmat4327
- [12] Seymour, K., Sheffield, J., Magleby, S. P., and Howell, L. L., 2019, Cylindrical Developable Mechanisms for Minimally Invasive Surgical Instruments. Proceedings of the ASME 2019 International Design Engineering Technical Conferences and Computers and Information in Engineering Conference. Volume 5B: 43rd Mechanisms and Robotics Conference. Anaheim, California, USA. August 18–21, 2019. V05BT07A054. ASME. https://doi.org/10.1115/DETC2019-97202
- [13] Spivack, M., 1975, A Comprehensive Introduction to Differential Geometry, Volume Three. Publish or Perish, Inc., 351.
- [14] Stoker, J. J., 1969, Differential Geometry. John Wiley and Sons, 114.
- [15] Wang, Y., Wang, C., Xiao, Y., Chen, B., Zhou, S., Guo, J., and Sun, M., 2016, Construction methodology for lip surface of a submerged inlet. Aerospace Science and Technology, **54**, 340-352.
- [16] Wilding, S. E., Howell, L. L., and Magleby, S. P., 2012, Spherical lamina emergent mechanisms. Mechanism and Machine Theory, 49, 187-197. doi.org/10.1016/j.mechmachtheory.2011.10.009
- [17] http://mathworld.wolfram.com/RigidMotion.html. Accessed 10/1/2016
- [18] http://www.mathwords.com/i/isometry.htm. Accessed 10/1/2016